17th Brazilian Congress of Thermal Sciences and Engineering
November 25th-28th, 2018, Águas de Lindóia, SP, Brazil

ENCIT-2018-0008
FORECASTING THE LENGTH OF THE UNDEVELOPED FLOW REGION IN THE INLET OF ASYMMETRIC BIFURCATIONS I

Flavio Peres Amado
Universidade Estacio de Sá, Rua Eduardo Luiz Gomes, 134 - Morro do Estado, Niterói - RJ, 24020-340
e-mails: flavioam@petrobras.com.br; fpamado@live.estacio.com.br
Mila Rosendarl Avelino
Universidade do Estado do Rio de Janeiro – UERJ, Cx. Postal 68503, Rio de Janeiro - RJ, 21945-970;
e-mail: mila.avelino@pq.cnpq.br
Jordana Colman
Universidade Federal do Rio de Janeiro – UFRJ, Centro de Tecnologia - Av. Horácio Macedo, 2030, Cidade Universitária, Rio de Janeiro - RJ, 21941-450
e-mail: jordanacolman@yahoo.com.br
Ediomedson Sales de Lucena
Narcisio Gragory dos Santos Mazzarela
Universidade Estacio de Sá, Rua Eduardo Luiz Gomes, 134 - Morro do Estado, Niterói - RJ, 24020-340
e-mails: ediomedson@hotmail.com, narcisio.gregory@gmail.com

Abstract. *Usually, equations for prediction of the undeveloped flow region length, presented in the literature for laminar regime in curved tubes, show that this extension is a function of the flow velocity (expressed by the Reynolds number), the pipe diameter (hydraulic diameter if section is not circular) and the curvature radius. Thus, an equation in the classical format is proposed to predict the length of the not fully developed flow region in asymmetric bifurcations of tubes with 20 mm in diameter. Simulations in finite difference method are performed for several angles and flow rates, as well as simulations in a commercial code, for comparison of results. Constants and exponents are calculated from the measurement of the region of interest in images generated in the models. The size of the region was larger as the fork angulation increased. Flow rate, within the range tested, was not as influential. A complementary work must be carried out in order to raise the effect of the diameter of the pipe and thus, reach a more adequate equation, which takes into account all the variables that matter to the phenomenon.*

Keywords: *flow development, bifurcations*

1. INTRODUCTION

Classically, Eq. (1), introduced by the basic literature (Fox and Mc Donalds, 1985, Bejan. A., 1993, Geankoplis, 1993, Incropera and Dewitt, 1998, Welty et al, 2001) to beginning students of Fluid Mechanics and Heat Transfer, shows the extent of the undeveloped flow region at the entrance of straight stretches of conventional piping. *Re* is the Reynolds Number. If the section is not circular, the diameter *D* shall be replaced by the hydraulic diameter, *Dh*.

$$L=0.05ReD \tag{1}$$

When talking about curved tubes, the first authors to study this region were Kreulegan and Beiji, 1937. Later, Austin and Seader, 1974, proposed Eq. (2), which is expressed under the shape of angular length.

$$\varphi = 49\left(De\frac{a}{R}\right)^{0.33} \tag{2}$$

In Eq. (2), *De* is the Dean Number, *a* is the pipe radius and *R* is the radius of curvature of the stretch.

Springer et al (2009) proposed an equation for toroidal and helicoid thin tubes, which considers that the length of the inlet region is a function of the Reynolds Number, the pipe diameter and the radius of curvature. Eq. (3) is valid within the constraint $0 \leq \mathrm{Re} \leq 400$; $0.25 \times 10^{-3}\ \mathrm{m} \leq 2a \leq 2 \times 10^{-3}\mathrm{m}$ and $4 \times 10^{-3}\ \mathrm{m} \leq R \leq 32 \times 10^{-3}\ \mathrm{m}$.

$$L=0.322\ (2R)^{0.31}\ Re^{0.59}\ (2a)^{0.76} \tag{3}$$

It is important to note that the equation is not homogeneous from the dimensional point of view, but the authors informed that it was the best way to express their results.

This equation was modified and tested for symmetric bifurcations of microchannels by Amado et al, 2018. The correlation presented as Eq. (4) was considered better suited to the range of bifurcation angles between 30 and 60 degrees, flow rates between 1.39 x 10^{-10} m^3/s and 5.56 x 10^{-10} m^3/s, with rectangular sectioned tubes, with widths between 80 and 200 μm and water flowing inside, under NTP conditions.

$$L=0.161\ (2R)^{0.31}\ Re^{0.59}\ Dh^{0.76} \tag{4}$$

As a bifurcation is not a curved stretch, *R* was considered to be the radius of curvature of an arc containing the feeder channel and one of the outlets, as shown in Fig. 1 (Amado et al., 2018) and it is given by de Eq (5).

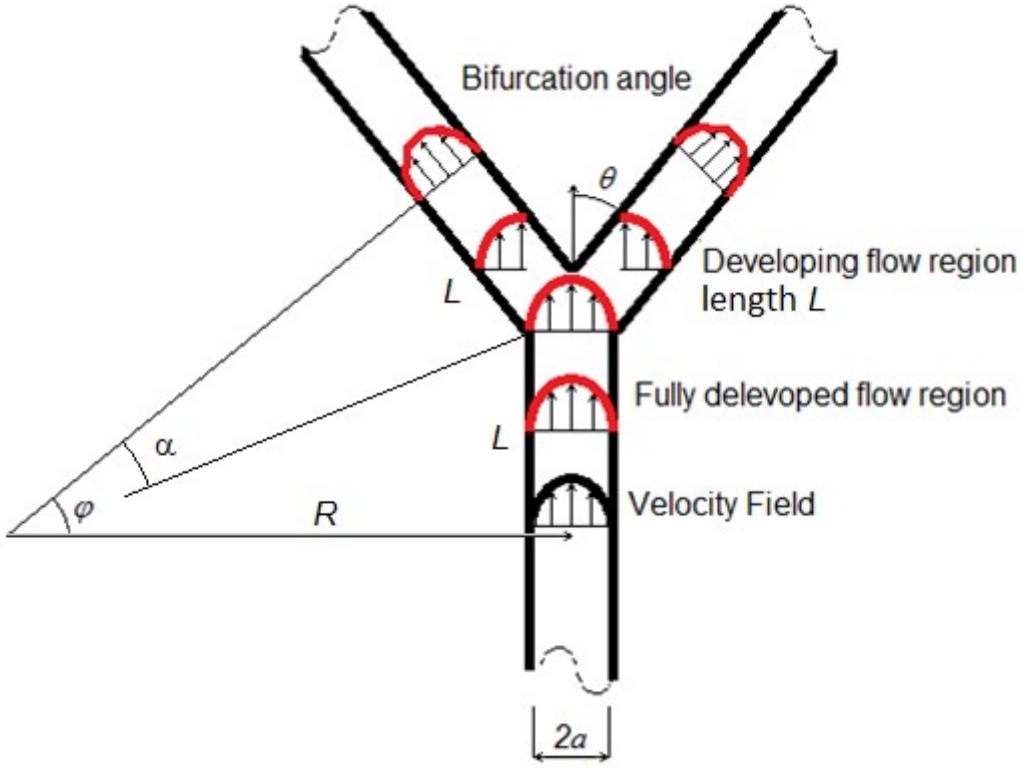

Figure 1. Sketch of a bifurcation in a rectangular sectioned microchannel with a half-angle θ, showing the developing flow region in the fork entrance (Amado et al, 2018).

$$R = \frac{1200{,}5 D_h Re^{0{,}66}}{\theta^2} \tag{5}$$

2. MATERIAL AND METHODS

The shape of the Eq. (3) proposed by Springer et all, 2009, was considered in this work as the ideal for calculating the size of the region of flow development in asymmetric bifurcations, made of circular sectioned tubes with diameter of 20 mm. Thus, generic format presented as Eq. (6), with constants *k*, *m*, *n* and *p,* must be found from results obtained in CFD analysis. In this case, *D* may be the diameter or the hydraulic diameter, as required.

$$L=k\ (2R)^m\ Re^n\ D^p \tag{6}$$

The fluid employed in this study was water under NTP conditions.

2.1 Simulation Strategy

Equations (7), (8) and (9) that govern the phenomenon were implemented in finite difference method, taking into account that the simplicity of the geometry allows a less robust numerical tool to be employed. Classical mass conservation and momentum equations were treated in Cartesian Coordinates and only two dimensions were considered, where x was the axial direction for any side of the bifurcation and z, the transversal one.

Equation for mass conservation:

$$\frac{\partial v_x}{\partial x} + \frac{\partial v_y}{\partial y} = 0 \tag{7}$$

x Momentum:

$$\rho\left(\frac{\partial v_x}{\partial t} + v_x\frac{\partial v_x}{\partial x} + v_z\frac{\partial v_x}{\partial z}\right) = \rho g_x - \frac{\partial P}{\partial x} + \mu\left(\frac{\partial^2 v_x}{\partial x^2} + \frac{\partial^2 v_x}{\partial z^2}\right) \tag{8}$$

z Momentum

$$\rho\left(\frac{\partial v_z}{\partial t} + v_x\frac{\partial v_z}{\partial x} + v_z\frac{\partial v_z}{\partial z}\right) = \rho g_z - \frac{\partial P}{\partial z} + \mu\left(\frac{\partial^2 v_z}{\partial x^2} + \frac{\partial^2 v_z}{\partial z^2}\right) \tag{9}$$

The simulation was performed using the methodology proposed in Amado et al (2018), considering as initial condition the Eq. (7) and velocity zero in the channel wall.

$$v_{axial} = \frac{2Q}{\pi r_i^4}(a^2 - r^2)\cos\pm\theta \tag{10}$$

In this equation, Q is the fluid flow rate, a is the inner radius of the pipe, r is the radius from the central line of the tube, according to which the velocity profile varies, and θ is one of the half angles $\theta 1$ and $\theta 2$ of the asymmetric bifurcation, as shown in Fig 2.

Just like Amado et al (2018), it was employed an uniform structured mesh by direction, which seemed to be easier for the case. After several iterations, the mesh chosen for both outlets was one of 1200 x 1200 cells (axial and transversal values). Combinations with more cells leaded to an excessive time of calculation without any difference in results. For the case of less cells, there were undesirable discontinuities in the final image.

The convergence criterion was 10^{-8}, compared to the relative error and the simulated time ranges were 1, 10, 20, 60 and 600 seconds, with steps of 0.00002 seconds. However, for periods longer than 1 second, results did not change and 1 second appeared to be adequate.

Two sets of simulations were performed. One with variation of angles and another with variation of flow rates, with dimensional characteristics according to data reported in Tab. 1 and 2.

The same simulations were performed in a commercial code, with the simple objective of comparing images by two different methods.

Another reason why the simulation in finite differences method was used consisted in the fact that it is not possible to use Eq. (10) as the initial condition of velocity into the commercial code. In this case, the software demands an initial velocity like a single and constant value. It is not possible to impose a parabolic input condition.

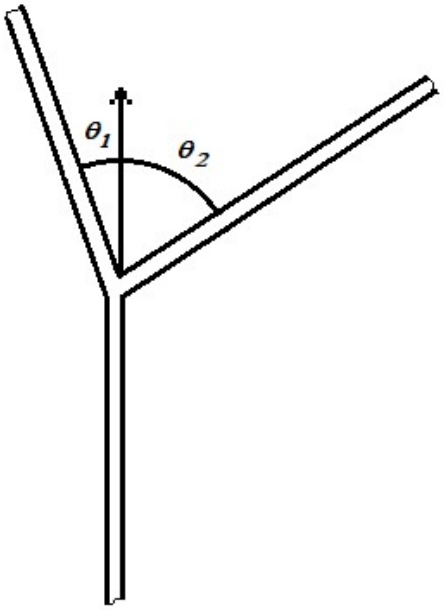

Figure 2. Sketch of asymmetric bifurcation, showing the angles θ_1 and θ_2 of each outlet.

Table 1. Conditions of flow in asymmetric bifurcations with the same pair of angles.

Channel	Dimensional data	Flow rate Q at the feeder channel inlet (m^3/s)
Inlet 1	Half-angles θ_1 *e* θ_2 as 45º and 30º, for bifurcations with 0.02 m in diameter and 0.9 m of length.	5.56×10^{-10}
Inlet 2		6.95×10^{-10}
Inlet 3		1.11×10^{-9}
Inlet 4		1.39×10^{-9}
Inlet 5		1.81×10^{-9}
Inlet 6		2.78×10^{-9}

Table 2. Variation of angles in asymmetric bifurcations with constant flow rate Q.

Channel	Half-angles	Flow rate Q Conditions
Outlet 1 left	5	1.39×10^{-9} m^3/s of flow rate Q at the feeder channel inlet, for bifurcations with 0.02 m in diameter and 0.9 m of length.
Outlet 1 right	15	
Outlet 2 left	15	
Outlet 2 right	30	
Outlet 3 left	30	
Outlet 3 right	45	
Outlet 4 left	45	
Outlet 4 right	60	
Outlet 5 left	60	
Outlet 5 right	75	
Outlet 6 left	75	
Outlet 6 right	90	

3. RESULTS AND DISCUSSION

Figure 3 and 4 show images obtained through the above-mentioned commercial code. Note that the image in Fig. 4 presents a "cubist" definition. This phenomenon happened due to the over-zooming of an image generated from the limit of capacity of mesh refinement of this software. The condition represented consists of half-angles θ_1 *and* θ_2 as 30º and 45º and flow rates $Q = 1.39 \times 10^{-9}$ m^3/s and 1.11×10^{-9} m^3/s. Fig 5 shows the corresponding image obtained by the finite difference method.

From the values shown in Tab. 1 and 2, Tab. 3 and 4 show the results achieved by measuring L in the generated images in the simulation performed using the finite difference method.

The best correlations found were Eq (11) for the case of asymmetric bifurcations with flow rate variation in the range of 5.56×10^{-10} and 2.78×10^{-9} m^3/s and constant pairs of half-angles 45º and 30º and Eq (12), for the case of constant flow rate and half-angle ranging from 5 to 90 degrees.

$$L=0.23(2R)^{-0.1}Re^{-0.24}D^{1.1} \quad (11)$$

$$L=0.006111(2R)^{-0.1}Re^{-1.44}D^{1.1} \quad (12)$$

These expressions are coherent from the dimensional point of view. In Eq. (3) and (4), the sum of the exponents m and p should be 1, since the exponent of L is 1, but Springer et al., 2009, did not care about the homogeneity of the formula proposed by them. As said initially, they only report that it represents the best match between measured and predicted values.

Figures 6 and 7 show the graphical comparison between the measured (Tab. 3 and 4) and predicted values, respectively by Eq. (11) and (12).

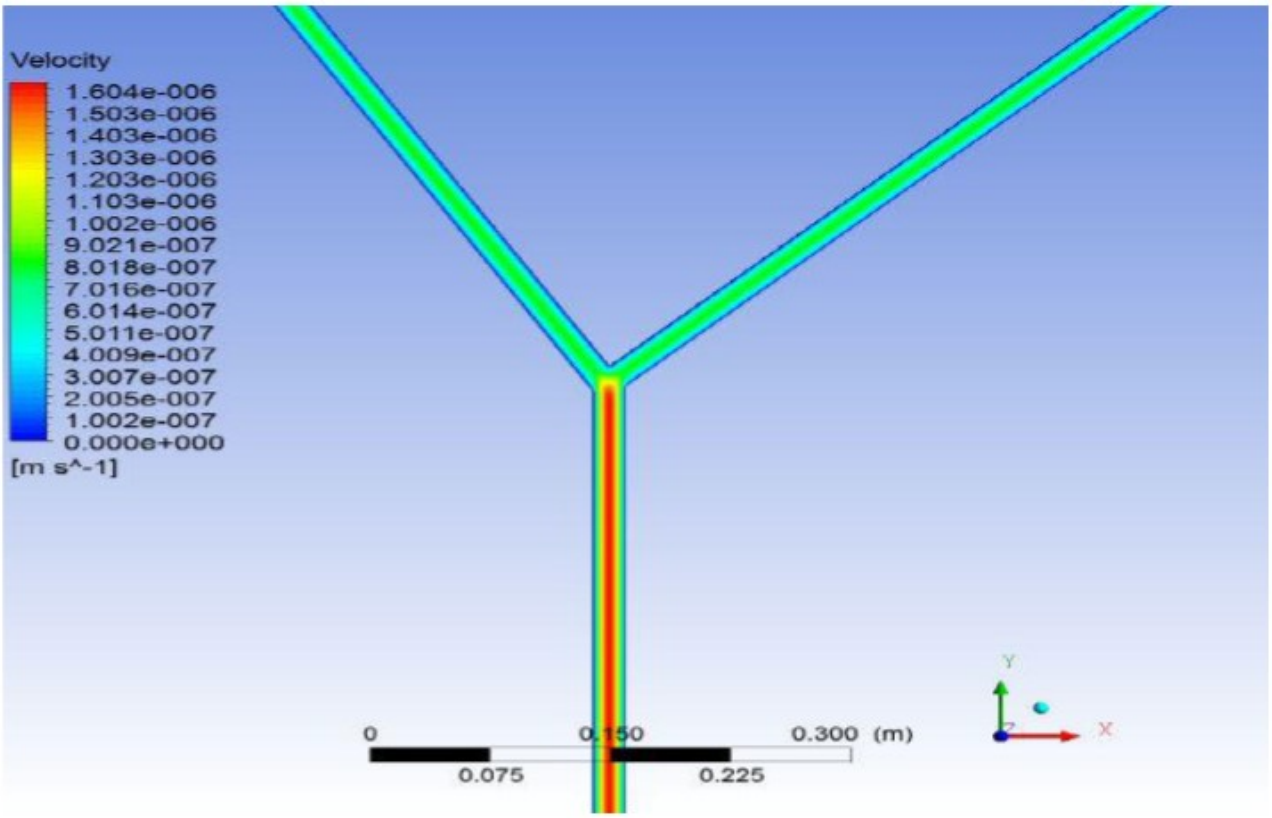

Figure 3. Simulation in commercial code, flow in a bifurcation with half-angles θ_1 *e* θ_2 as 30º and 45º, flow rate Q 1.39 x 10^{-9} m^3/s, for inlet and outlets with 0.02 m in diameter and 0.9 m of length.

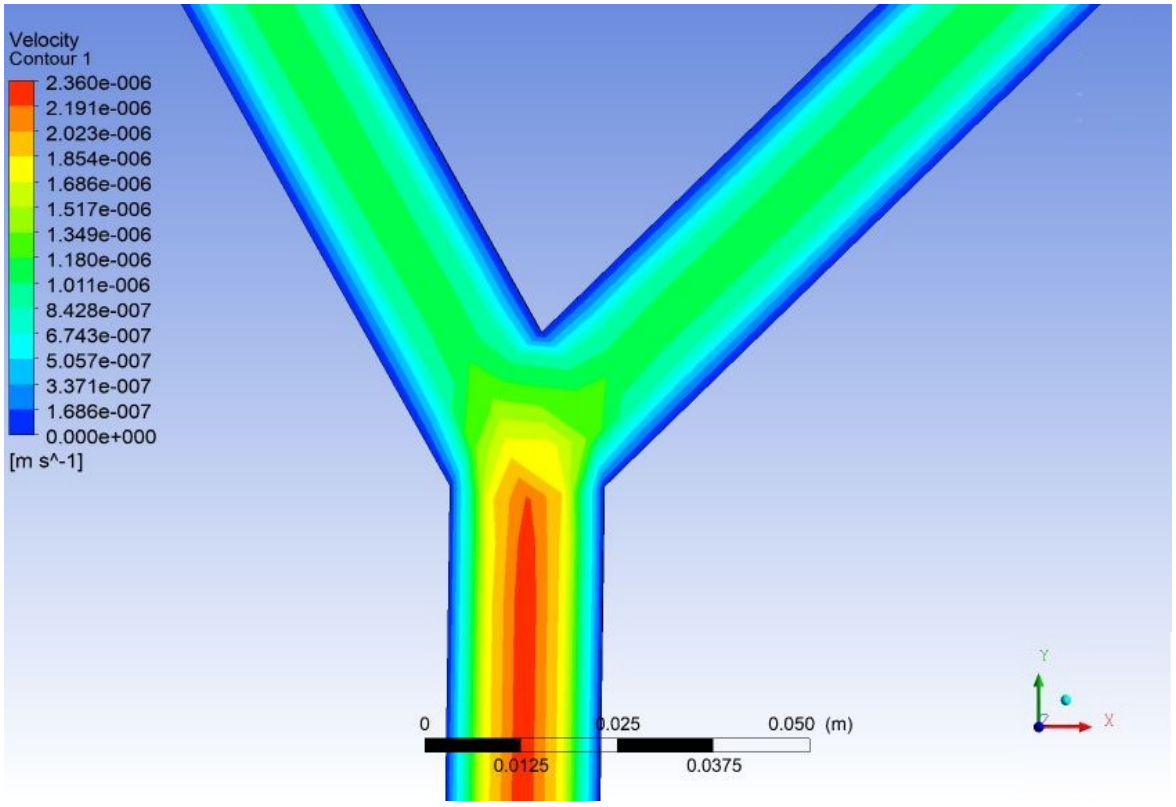

Figure 4. Simulation in commercial code, flow in a bifurcation with half-angles θ_1 *e* θ_2 as 30º and 45º, flow rate Q 1.11 x 10^{-9} m^3/s, for inlet and outlets with 0.02 m in diameter and 0.9 m of length.

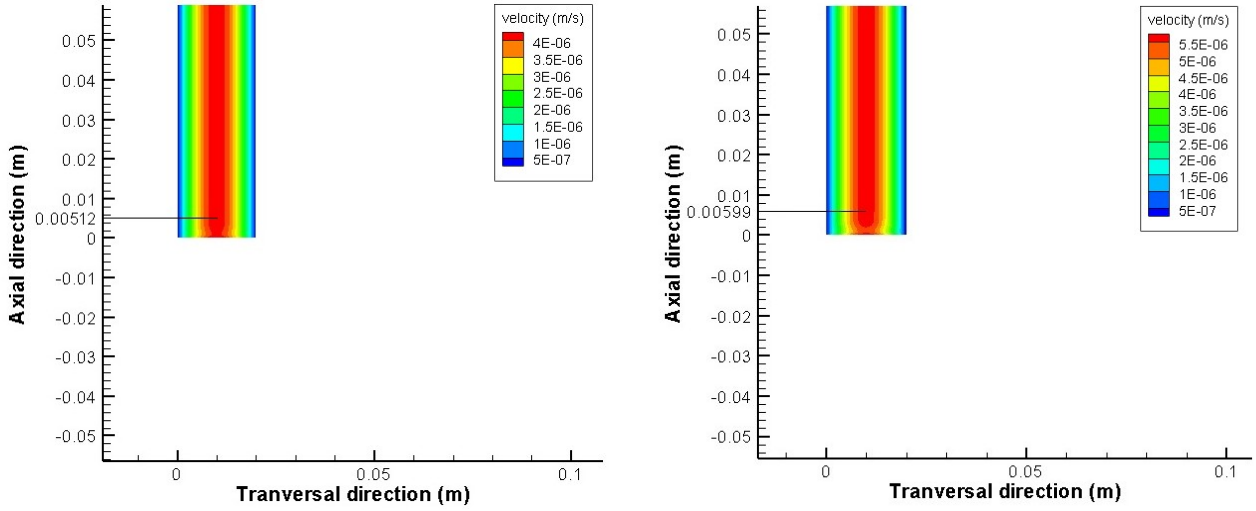

Figure 5. Simulation in finite difference method, flow in a bifurcation with half-angles θ_1 as 30º *at right and* θ_2 as 45º at left, flow rate Q 1.39 x 10^{-9} m^3/s, for outlets with 0.02 m in diameter and 0.9 m of length. In these images were measured the regions of interest.

Table 3. Length L of the region of flow development, measured in the images generated in simulations, with variation of flow rate Q.

Channel	Length measured
Outlet 1 left	0.00453
Outlet 1 right	0.00433
Outlet 2 left	0.00552
Outlet 2 right	0.00477
Outlet 3 left	0.00519
Outlet 3 right	0.00446
Outlet 4 left	0.00559
Outlet 4 right	0.00375
Outlet 5 left	0.00512
Outlet 5 right	0.00362
Outlet 6 left	0.00453
Outlet 6 right	0.00387

Table 4. Length L of the region of flow development, measured in the images generated in simulations, with angular variation.

Channel	Length measured
Outlet 1 left	0.00303
Outlet 1 right	0.00441
Outlet 2 left	0.00379
Outlet 2 right	0.00455
Outlet 3 left	0.00512
Outlet 3 right	0.00599
Outlet 4 left	0.00558
Outlet 4 right	0.00633
Outlet 5 left	0.00665
Outlet 5 right	0.00735
Outlet 6 left	0.00574
Outlet 6 right	0.00623

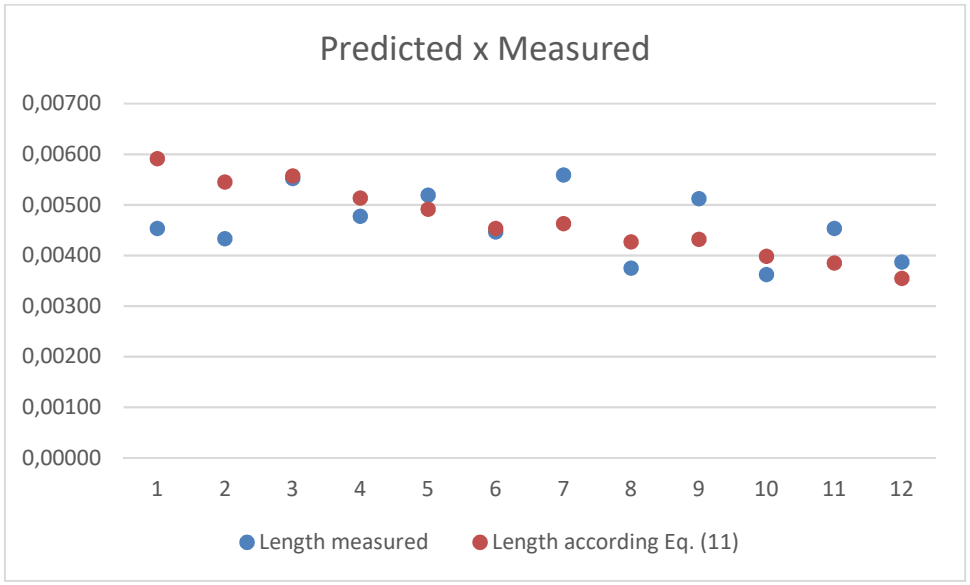

Figure 6. Graphical comparison between values measured by CFD and values predicted by Eq. (11).

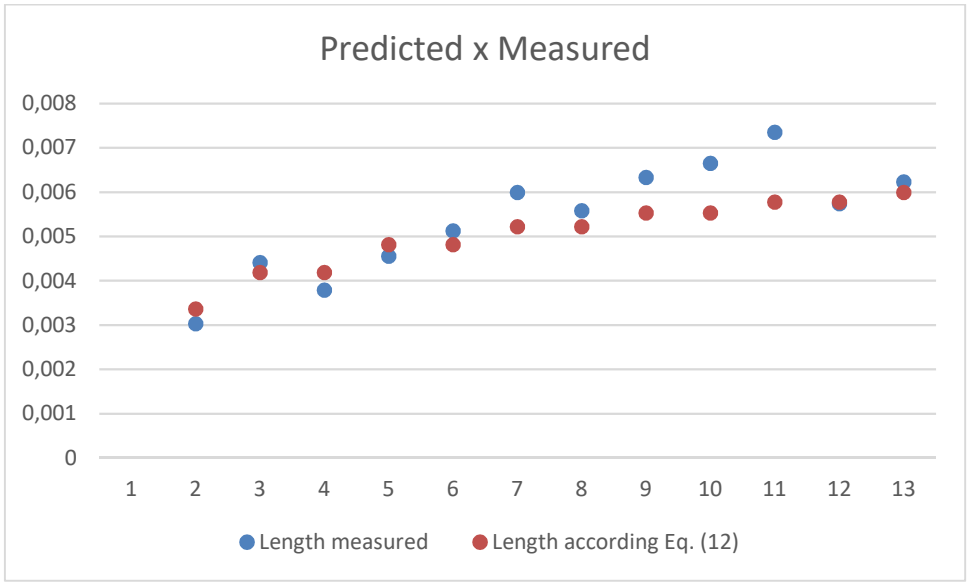

Figure 7. Graphical comparison between values measured by CFD and values predicted by Eq. (12).

These equations allow to conclude that the greater the radius of curvature of the arch containing the bifurcation (or the smaller the bifurcation half-angle). the smaller the extent of the not fully developed flow region.

The influence of flow rate. within the range of values employed. was not as effective as it could be supposed, however, the trend shown is that the lower the flow rate, the shorter the length of the flow development.

These conclusions are corroborated by Pozrikidis. 2012. which worked with zero-angled bifurcations.

3.1 The relevance of the length *L*

In order to verify if the length of the not fully developed stretch is long enough to be taken into account. Garimella S.V. And Singhal , 2004, and Steinke. and Satish, 2005,applied Eq. (13). The objective was to verify if the flow can be considered fully developed for the entire length of the outlet.

$$x^+ = \frac{L}{D_h Re} \tag{13}$$

For a value greater than x+ = 0.05. the entire flow can be considered fully developed. As per those cases presented in Tab. 3 and 4. values of x+ are presented in Tab. 5 and 6.

Table 5 – Values of x+ for each values of Length *L* for flow rate *Q* variation

Channel	*L* (m)	*D* (m)	*Re*	*x*+
Outlet 1 left	0.00453	0.02	0.017610	12.86202
Outlet 1 right	0.00433		0.017610	12.29417
Outlet 2 left	0.00552		0.022012	12.53834
Outlet 2 right	0.00477		0.022012	10.83477
Outlet 3 left	0.00519		0.035220	7.36798
Outlet 3 right	0.00446		0.035220	6.33164
Outlet 4 left	0.00559		0.044025	6.34867
Outlet 4 right	0.00375		0.044025	4.25895
Outlet 5 left	0.00512		0.057232	4.47299
Outlet 5 right	0.00362		0.057232	3.16254
Outlet 6 left	0.00453		0.088050	2.57240
Outlet 6 right	0.00387		0.088050	2.19762

Table 6 – Values of x+ for each values of Length L for angular variation

Channel	*L* (m)	*D* (m)	*Re*	*x*+
Outlet 1 left	0.00303	0.02	0.04402	3.44123
Outlet 1 right	0.00441			5.00852
Outlet 2 left	0.00379			4.30438
Outlet 2 right	0.00455			5.16752
Outlet 3 left	0.00512			5.81488
Outlet 3 right	0.00599			6.80296
Outlet 4 left	0.00558			6.33732
Outlet 4 right	0.00633			7.18911
Outlet 5 left	0.00665			7.55254
Outlet 5 right	0.00735			8.34754
Outlet 6 left	0.00574			6.51903
Outlet 6 right	0.00623			7.07553

The rather small length of the developing flow region found for the bifurcations studied in this paper, as well as its verification through Eq. (13), show that the flow can be considered fully developed after the bifurcations, for the entire length of both side, in all devices studied herein. Low values of *L* are expected for minicanals and microchannels, according to results of Garimella S.V. And Singhal, 2004, and Steinke. and Satish, 2005. The values of x+ shown in Tab. 5 and 6 also indicate very low *L* values for diameter of 20 mm. A complementary study with bifurcations of larger diameters is recommended, for the better understanding of the relevance of the flow development region in these cases.

4. CONCLUSION

Equations for predicting the length of the not fully developed flow region at the entrance of asymmetric bifurcations with diameter of 20 mm were presented. They were postulated in the classic format employed in the specialized literature. Constants and exponents were drawn from measurements in CFD analysis, varying flow rates and angles.

Results allowed to conclude that the regions of interest are larger, the bigger the half-angles of the bifurcation. Within the flow rate range of 5.56×10^{-10} m^3/s and 2.78×10^{-9} m^3/s, with ralf-angles 45º and 30º, it was not possible to notice a greater influence of this variable on the length of the undeveloped flow region.

The measured length values were so small that the flow could be considered to be developed along the entire length of the simulated bifurcations.

A complementary work. with variation of diameters must be carried out, in order to raise the effect of this variable in the region of interest and to obtain a unique equation, with broad coverage.

5. ACKNOWLEDGEMENTS

The authors acknowledge “Programa Pesquisa Produtividade - Universidade Estácio de Sá” for funding the research.

6. REFERENCES

Amado, F. P., Avelino. M. R., Colman, J., Lucena, E. S., Mazzarela, N. G. S., 2018. “Developing Flow in the Inlet Region of Bifurcations in Microchannels with Symmetric Angulation”. to be published in the Proceedings of the CONEM 2018.

Austin, L. R., Seader, J. D., 1974. “Entry Region for Steady Viscous Flowing Coiled Circular Pipes”. American Institute of Chemical Engineers. vol 20. pp 820–822.

Bejan, A., 1993. “Heat Transfer”. John Wiley & Sons. Inc., p. 292.

Fox and Mc Donald., 1985. “Introduction to Fluid Mechanics”. Jonh Wiley & Sons, 3a ed.

Garimella S.V. And Singhal,V., 2004. “Single-Phase Flow and Heat Transport and Pumping Considerations in Microchannel Heat Sinks”. Heat Transfer Engineering, 25:1, 15-25, DOI:10.1080/01457630490248241.

Geankoplis, C.J., 1993. “Transport Processes and Unit Operations”. 3rd Edition. Prentice-Hall, Inc

Incropera, F.P. e DeWitt, D.P., 1998, “Fundamentos da Transferência de Calor e de Massa”. 4a Edição. LTC Livros Técnicos, Rio de Janeiro

Keulegan, G. H., Beiji. K. H., 1937. “Pressure Losses for Fluid Flows in Curved Pipes”. Journal of Research of NIST. vol 18. pp 89–144.

Pozrikidis C, 2012. “Passage of a liquid drop through a bifurcation”. Engineering Analysis with Boundary Elements 3. pp 693–103.

Springer, F., Carretier, E., Veyret, D., Moulin, P., 2009. “Developing Lengths in Woven and Helical Tubes with Dean Vortices Flows”. Engineering Applications of Computational Fluid Mechanics. 3:1. 123-134. DOI:10.1080/19942060.2009.11015259.

Steinke, M. E., and Satish G. K. , 2005. “Single-phase liquid friction factors in microchannels”. 3rd International Conference on Microchannels and Minichannels. American Society of Mechanical Engineers ASME.

Welty, J.R. (Ed.), Wicks, C.E., Wilson, R.E., Rorrer, G., 2001. “Fundamentals of Momentum, Heat, and Mass Transfer”. 4th Ed. John Wiley & Sons.

7. RESPONSIBILITY NOTICE

The authors are the only responsible for the printed material included in this paper.